Theory and Practice of Science and Technology
2025, VOL. 6, NO. 2, 163-170
DOI: 10.47297/taposatWSP2633-456931.20250602

Transition Dynamics for a bistable membrane-type acoustic metamaterial system

Xia Feng[1], Jinqian Feng[1,2]*, Jin Su[1,2], Qin Guo[1], Youpan Han[1]

[1]School of Science, Xi'an Polytechnic University, Xi'an, 710048, China;

[2]Xi'an International Science and Technology Cooperation Base For Big Data Analysis;and Algorithms, Xi'an, 710048, China.

ABSTRACT
Transition phenomena between bistable states induced by noise fluctuations have emerged as a critical topic in ensuring the reliability of complex systems. These transitions cause abrupt jumps between states, often compromising the structural stability of metamaterials. This paper investigates the transition dynamics in an acoustic metamaterial model. The Onsager-Machlup action functional theory provides a potential way to capture the most probable transition path within a small tube, governed by the Euler-Lagrange equation. Solving this boundary-value problem efficiently presents a significant challenge. To address this, we employ the physics-informed neural networks(PINNs) method enhanced with a combined optimizer. Our results demonstrate that the AdamW+LBFGS optimization approach consistently achieves the higher accuracy and the faster convergence. Additionally, we analyze the effects of transition time and noise fluctuations on the transition path. The findings reveal that noise fluctuations can trigger transitions, altering the transition path through various manifold orientations. The minimum probable transition time is also derived numerically.

KEYWORDS
nonlinear dynamics; acoustic metamaterial model; Onsager-Machlup action functional,; the most probable transition path; physics informed neural networks

1 Introduction

Membrane-type acoustic metamaterials(MTAM) have attracted extensive attention in physics and acoustic engineering due to their good sound insulation, low quality and low construction cost. It is anticipated that dynamic phenomena including resonance, transition, bifurcation and chaos will offer a novel mechanism for acoustic wave propagation in acoustic metamaterials[1-2]. This is expected to result in low-frequency, broadband and efficient absorption. By gluing a mass block in the center of the stretched membrane, MTAM with low-frequency absorption characteristics was designed and produced. It has a narrow band of low-frequency absorption, which is essentially a narrow band. The narrow absorption bandwidth is greatly limited in practical applications, and the vibration response can capture the bandwidth problem well. Therefore, we consider significant changes or conversion of acoustic response due to random perturbations in MTAM models. With external conditions changing, such as temperature, pressure or external excitation frequency, these changes lead the material to transition from one stable state to another. This transition can bring significant changes in acoustic properties, such as switching from one acoustic transmission mode to one acoustic absorption mode, or from one phase to another.

Stochastic dynamical systems(SDS) are employed to simulate complex phenomena in physics[3], biology[4], chemistry[5], finance and engineering[6]. Those systems can maintain a stable state under certain parameter conditions, but the occurrence of external noise fluctuations will destroy this stability, resulting in a sudden critical transition of the system. These transitions are the reason for the metastable phenomena observed in the system, such as stochastic acoustic metamaterials[7], gene regulatory networks[8], climatic changes[9] and chemical reaction systems[10]. Therefore, quantifying the transition dynamics contributes to capturing the complex evolution of the system.

The transition dynamics are investigated by employing both numerical and approximate analytical methods. The former includes techniques such as Monte Carlo[11] and the adaptive minimum action method[12], while the latter encompasses Freidlin-Wentzell(FW) [13-14] and Onsager-Machlup(OM) theory[15]. Numerical methods offer precise calculations, they tend to become increasingly costly as the dimensions of the research problem increase, resulting in a dimension disaster. In contrast, approximate analytical methods can provide an approximate expression for the transition dynamics, which can often overcome the dimension limitation. For small noise cases, FW theory provides a framework to measure transition probability and the most probable transition path. Based on the large deviation principle, Wei and Duan[16] described the most probable transition path as an optimal control problem. Alternatively, it is hoped that the jump will be completed within the specified time region. In order to achieve this, it is necessary to increase the intensity of the noise and gain sufficient energy in the noise to escape from the stable state as soon as possible. In such situations, the Onsager-Machlup theory has attracted more attention. Onsager and Machlup[17] first derived the OM function of the diffusion process with linear drift and constant diffusion coefficient. For the solution process of stochastic differential equation(SDE) driven by Gaussian noise, OM theory has been extensively investigated in[18-20]. Since then, these studies have been extended to Levy noise[21].

In this paper, we investigate the transition dynamics of a MTAM system. Based on the Onsager-Machlup functional theory, PINNs[22] is applied to numerically solve Euler-Lagrange equation, which characterizes the most probable transition path. Compared with the existing methods[23-25], the typical PINNs approach can easily calculate the most probable transition paths. However, the typical PINNs method for the acoustic metamaterial model exhibits a relatively poor convergence performance, so we introduce the PINNs method with a combined optimizer to solve the Euler-Lagrange equation. Furthermore, we also explore the influence of transition time and noise fluctuation on transition paths. Noise plays an important role in the dynamics[26-27], which can induce the occurrence of transition dynamics.

The remainder of the paper is organized as follows: In Section 2, a stochastic model is considered to examine the dynamic behaviour of acoustic metamaterials. In accordance with the OM theory, the Euler-Lagrange equation that is satisfied by the most probable transition path is derived. In Section 3, by employing the variational principle, we apply the PINNs to solve the corresponding Euler-Lagrange equation to obtain the most probable transition path. Moreover, we discuss the effect of noise fluctuation and transition time on the transition dynamics. The results show that noise fluctuations can trigger transitions and change the transition paths through various manifold orientations. The minimum possible transition time is also derived by numerical methods. The conclusion emphasizes strengths and limitations of our research in Section 4.

2 Model and Methodology

2.1 Membrane-type acoustic metamaterial model

Consider a typical MTAM model, whose specific structure is shown in Fig.1. In Fig.1, the yellow small circle represents the magnetic mass block, which is affixed to the central position of the flat plane. An acoustic metamaterial comprising a magnetic mass block and a flat plate is formed. A magnetic field is positioned on the upper and lower sides of the plate-type acoustic metamaterial magnetic mass block to sustain the coupling effect between the magnetic mass block and the magnetic field. When the mass block oscillates, it is influenced by the elastic force on the plate and the magnetic field attraction concurrently. However, the elastic force exerted by the plate is consistently greater than the magnetic field attraction, ensuring the optimal operation of the system.

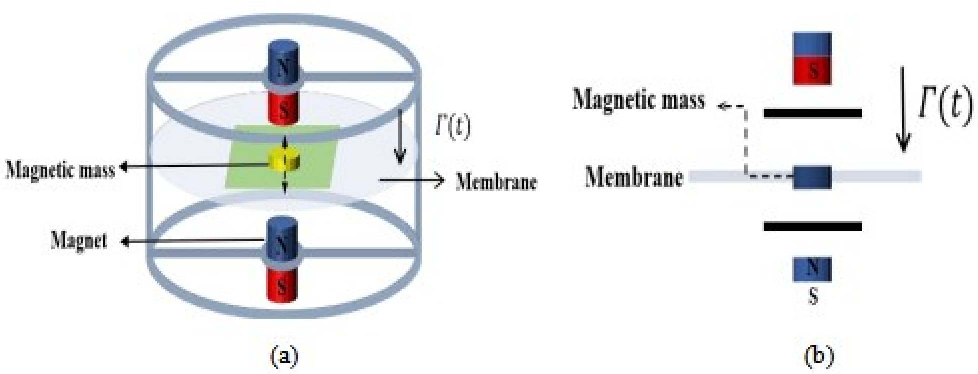

Figure 1 Diagrams of the membrane-type acoustic metamaterial. (a)Three dimensional and (b)side plane.

Under the combined action of the attraction of the magnet and the incident sound wave, the motion law of the membrane vibrating and bending over time can be described by the following differential equation[7]

$$M\ddot{x}(t)+(2\zeta_i\omega_i M+\rho c\beta^2 S)\dot{x}(t)+(K+\frac{\rho c^2\beta^2 S}{D}+k_1)x(t)+k_3x^3(t)=2\beta Sp_{in}(t), \tag{1}$$

where $\ddot{x}$, $\dot{x}$ and x represent the acceleration, velocity and displacement variables of the membrane during vibration, respectively. Let $M=M_i/\phi_{i,0}^2, K=M\omega_i^2, \beta=\langle\phi_i\rangle/\phi_{i,0}$,

in which $\phi_{i,0}$ and $\langle\phi_i\rangle$ denote the maximum value and surface average value of the shape of the *i*-th mode, respectively. While M_i, ζ_i and ω_i correspond to the modal mass, the modal damping ratio, and the natural frequency of the *i*-th modal shape, respectively. ρ and c refer to air density and the sound velocity, respectively. S signifies the area of the plane plate and D symbolizes the depth of the closed air cavity. k_1, k_3 represent linear and nonlinear stiffness coefficients derived from magnetic forces, respectively. The p_{in} is considered to be the power spectrum of the sound wave incident on the absorber, which describe the intensity of the sound wave.

With a specified initial displacement x_0, we apply the operation of multiplying both sides of Eq.(1) by $1/Mx_0$. Let $x(t)=X(t)/x_0$, then $\dot{x}(t)=\dot{X}(t)/x_0$, $\ddot{x}(t)=\ddot{X}(t)/x_0$. Consequently, the dimensionless equation of the system is

$$\ddot{x}+\alpha_1 x+\alpha_2\dot{x}+\alpha_3 x^3=\Gamma(t), \tag{2}$$

where $\alpha_1=(K+\frac{\rho c^2\beta^2 S}{D}+k_1)/M$, $\alpha_2=(2\zeta_i\omega_i M+\rho c\beta^2 S)/M$ and $\alpha_3=k_3 x_0{}^2/M$

represent stiffness, damping coefficients and nonlinear stiffness coefficients, respectively. Suppose that the force $\Gamma(t)=2\beta Sp_{in}(t)/Mx_0$ between the power spectrum of the incident sound wave and the time scale in Eq.(2) is a Gaussian noise $W(t)$.

Let $y=dx/dt$, consider the interference of noise in the displacement direction, system (2) is converted into a more general form

$$\begin{aligned} dx&=ydt+\sigma_1 dW_t^1,\\ dy&=(\alpha_1 x-\alpha_3 x^3-\alpha_2 y)dt+\sigma_2 dW_t^2, \end{aligned} \tag{3}$$

where σ_1 and σ_2 represent displacement noise and velocity noise, dW_t^1 and dW_t^2 denote independent increments of the standard Gaussian process. Given parameter values $\alpha_1=1,\alpha_2=1,\alpha_3=1$, the deterministic system (i.e. $\sigma_1=\sigma_2=0$) has two stable points $SN1(-1,0)$, $SN2(1,0)$ and an unstable point $US(0,0)$, and its potential function is $V(x,y)=-xy+\frac{1}{2}y^2+x^3y$, see Fig.2. Fig.3 shows the phase diagram for one sample path of system (3). From Fig.3, it can be seen that the system exhibits a tendency to transition between two equilibrium states.

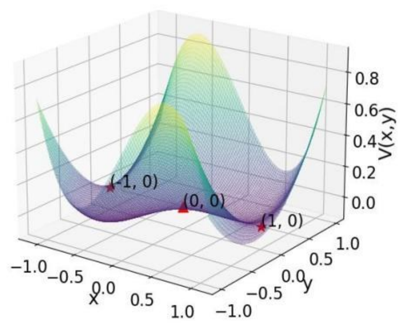

Figure 2 Potential function of system (3).

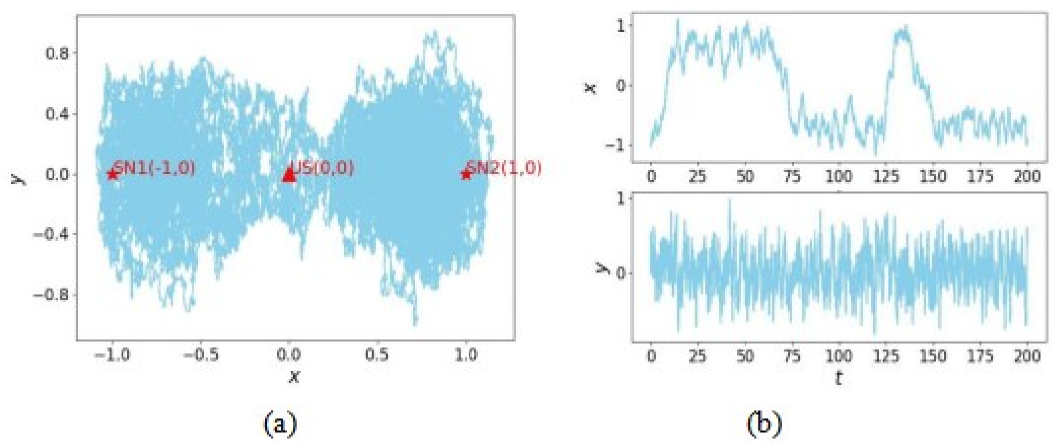

Figure 3 (a)Phase diagram of system (3) with two stable points (−1,0),(1,0) and an unstable saddle (0,0). (b)Time history diagram.

2.2 Onsager-Machlup theory

A brief introduction to the Onsager-Machlup theory to describe the most probable transition path[15]. Consider the following stochastic differential equation in R^m

$$dX(t)=f(X(t))dt+\sigma dW_t, \tag{4}$$

the initial value is $X(0)=x_0\in R^m$, where $f:R^m\to R^m$ is a regular function, $\sigma=diag(\sigma_1,\sigma_2,\cdots\sigma_m)$ is a matrix-valued function, $W(t)$ denotes a Brownian motion in R^m.

It is possible to consider the probability of a solution path on a small tube. The Onsager-Machlup theory of SDS (4) provides an approximation of probability

$$\mathbb{P}(\{\|X-z\|_T \le \delta\}) \propto C(\delta,T)\exp\{-S_{OM}(z,\dot{z})\}, \tag{5}$$

where ε is positive and sufficiently small, $C(\varepsilon,T)=\mathbb{P}(\{\|W\|_T \le \varepsilon\})$ denotes the probability of Brownian motion in the ε-tube. $\|\cdot\|_T$ represents the uniform norm of all continuous function spaces within the time interval $[0,T]$, while z is the function in this space. Furthermore, the Onsager-Machlup action functional S_{OM} is defined as

$$S_{OM}(z,\dot{z})=\frac{1}{2}\int_0^T [\dot{z}-f(z)][\sigma\sigma^T]^{-1}[\dot{z}-f(z)]+\nabla\cdot f(z)dt. \tag{6}$$

For simplicity, the Onsager-Machlup action functional can be considered as an integral of the Lagrange function

$$S_{OM}(z,\dot{z})=\frac{1}{2}\int_0^T L(z,\dot{z})dt, \tag{7}$$

where the Lagrangian $L(\cdot,\cdot)$ may be conceived as the integrand function of the Onsager-Machlup action functional S_{OM}. The minimum value of the action functional (6) represents the maximum probability of the solution path on the tube. By minimizing the Onsager-Machlup action functional, it is possible to investigate the most probable transition path.

For this purpose, the transition path is constrained to two differentiable functions with fixed initial and final states. In accordance with the variational principle, it can be shown that the most probable transition path of the SDE (3) is subject to the Euler-Lagrange equation

$$\frac{d}{dt}\frac{\partial}{\partial \dot{z}}L(z,\dot{z})=\frac{\partial}{\partial z}L(z,\dot{z}), \tag{8}$$

with initial state $z(0)=z_0$ and final state $z(T)=z_T$. Frequently, z_0 and z_T are selected as the two metastable states.

In essence, the Euler-Lagrange equation (8) for our system can be regarded as a second-order ordinary differential equation of two dimensions

$$\ddot{z}=g(z,\dot{z}), \tag{9}$$

where g is associated with the drift term f and diffusion term σ in stochastic differential equation (4).

For system (3) i.e. $\sigma=diag\{\sigma_1,\sigma_2,\cdots\sigma_m\}$, let $z=(x,y)$, then the Euler-Lagrange equation corresponding to the Onsager-Machlup action functional (6) is

$$\begin{aligned}
\ddot{x}&=\frac{\partial f^1(x,y)}{\partial x}\dot{x}+\frac{\partial f^1(x,y)}{\partial y}\dot{y}-(\dot{x}-f^1(x,y))\frac{\partial}{\partial x}f^1(x,y)\\
&-\frac{\sigma_1^2}{\sigma_2^2}(\dot{y}-f^2(x,y))\frac{\partial}{\partial x}f^2(x,y)+\frac{\sigma_1^2}{2}\frac{\partial}{\partial x}a(x,y),\\
\ddot{y}&=\frac{\partial f^2(x,y)}{\partial x}\dot{x}+\frac{\partial f^2(x,y)}{\partial y}\dot{y}-(\dot{y}-f^2(x,y))\frac{\partial}{\partial y}f^2(x,y)\\
&-\frac{\sigma_2^2}{\sigma_1^2}(\dot{x}-f^1(x,y))\frac{\partial}{\partial y}f^1(x,y)+\frac{\sigma_2^2}{2}\frac{\partial}{\partial y}a(x,y).
\end{aligned} \tag{10}$$

where $f^1(x,y)=y$ and $f^2(x,y)=a_1x-a_3x^3-a_2y$ represent drift function, more details see Appendix A.

3 Numerical experiment

The PINNs method represents an effective tool for solving boundary value problems. In this section, we utilize the PINNs method with a combined optimizer to solve Eq.(10) to obtain the approximate solution of the transition path. This approach effectively captures and simulates complex physical processes by constructing neural networks and employing their governing equations as a component of the loss function.

Given the data set $\{(t_j,z_j)\}_{j=1}^M$, where $t_j\in[0,T]$, $z_j=z(t_j)$, $z(t)=(x(t),y(t))$, the boundary data set are taken as $\{(0,z_0),(T,z_T)\}$. Consequently, the empirical loss function is defined as

$$\begin{aligned}
\mathbf{H}(\theta)&=\frac{1}{M}\sum_{j=1}^{M}\left\|\ddot{z}(t_j)-g(z(t_j),\dot{z}(t_j))\right\|^2\\
&+\lambda(\left\|z(0)-z_0\right\|^2+\left\|z(T)-z_T\right\|^2),
\end{aligned} \tag{11}$$

where λ is a positive constant that balances residual losses and boundary losses. $\theta=(\sigma,\square)$, where σ and $\square$ represent the noise amplitude and network parameters, respectively. Eq.(11) can be reformulated as the following optimal problem

$$\theta^*=\arg\min_\theta \mathbf{H}, \tag{12}$$

the following simulation employs the PyTorch framework, a fully connected neural network with 2 hidden layers, comprising 20 neurons per layer, and a tanh activation function was constructed for training. The weights are initialized with truncated normal distribution and the biases are initialized to zero.

The traditional optimizer exhibits a slow convergence effect and low precision for system (3). We compare the gradient-based optimizer AdamW and SGD with the combination optimizer AdamW + LBFGS. The result is shown in Fig. 4. It is observed that the AdamW and SGD optimizer converge slowly, whereas the LBFGS optimizer demonstrates a rapid convergence after 6000 iterations, which shows the superiority of AdamW+LBFGS combination. Accordingly, the optimizer for subsequent training uses AdamW+LBFGS with a learning rate of $10^{-3}$to train the loss function.

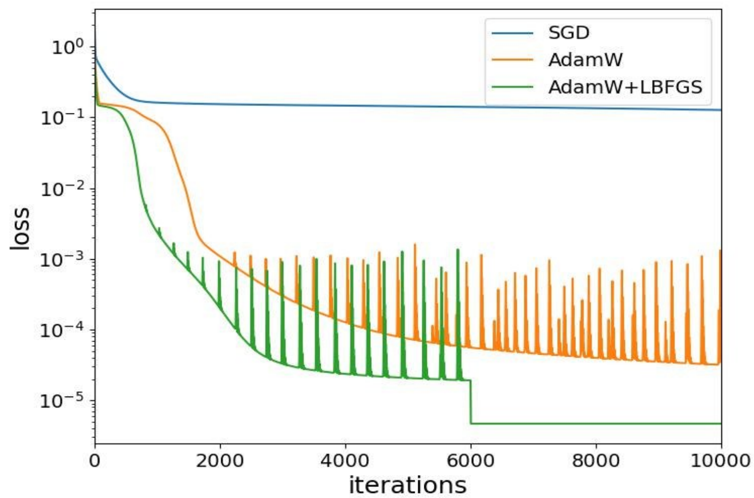

Figure 4 The loss under different optimizers, with the AdamW optimizer optimized for 6000 iterations followed by optimization using the LBFGS optimizer.

In order to demonstrate the most probable transition path, we fix$T = 2$, $\sigma_1 = 0.5$,$\sigma_2 = 0.3$. Fig.5 illustrates the vector field of system (3), as well as five sample paths (colorful) and the most probable transition path (black). Obviously, the domain of attraction is separated by the stable manifold of the unstable saddle point US(0,0). We employ the approximate Markov bridge method[28], which is an effective technique for capturing sample transition paths. Setting $\sigma_1 = 0.5$,$\sigma_2 = 0.3$, the result is shown in Fig.5(b). The sample paths are observed to be concentrated near the most probable transition path. While the most probable transition path may be identified as the maximum probability around their adjacent sample paths, it is important to note that these paths do not necessarily represent the actual sample paths of the particles.

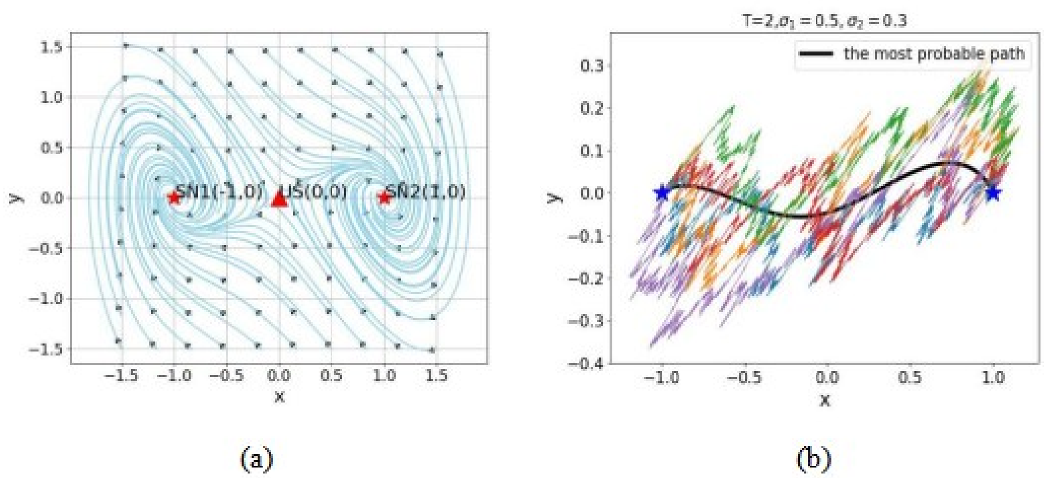

Figure 5(a) Vector field of system (3). (b) Most probable transition path (black) and five sample paths (colorful).

3.1 The effect of the noise amplitude

In a stochastic acoustic metamaterial, the presence of noise is a significant factor for inducing transition. Firstly, fixed $T = 2$, the most probable transition paths with different noise amplitudes are discussed, as shown in Fig.6. We analyze the results of Fig. 6(a), an interesting phenomenon shows that when the time and noise amplitude $\sigma_1$are fixed, with the increase ofσ_2, the shape of the most probable transition path gradually changes from a double potential well to an arch. Furthermore, it is probable that the most path will transition from the manifold orientations beneath the saddle point US

(0,0) to the manifold orientations that is situated above it. On the contrary, the time and noise amplitude$\sigma_2$are fixed, with the increase ofσ_1, the shape of the most probable transition path gradually changes from arch to double potential well, and it is highly probable that the most path will transition from the manifold orientations situated above the saddle point US(0,0) to the manifold orientations located below the saddle point, see Fig.6(b).

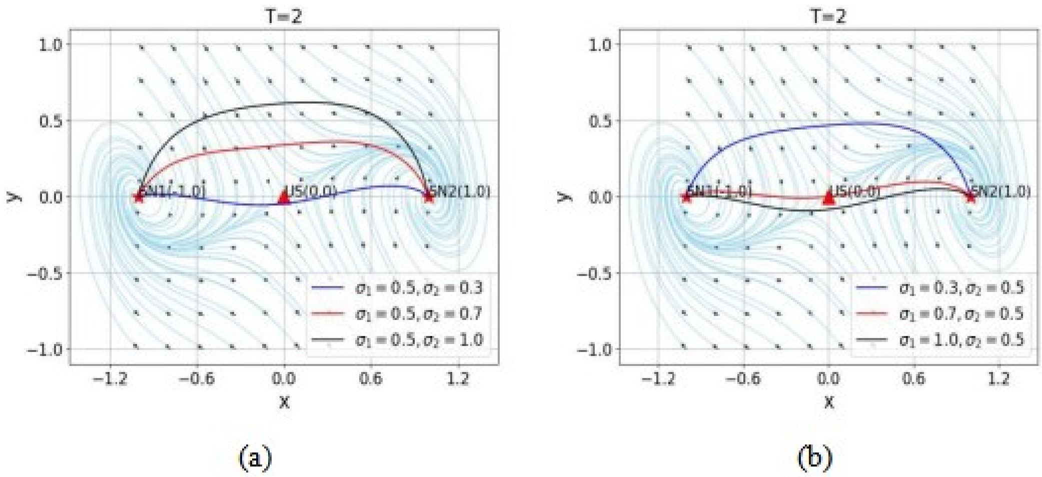

Figure 6 Fixed$T = 2$, the most probable transition paths under different noise amplitudes
(a) Fixed$\sigma_1 = 0.5$and different values$\sigma_2 = 0.3,0.7,1.0$. (b) Fixed$\sigma_2 = 0.5$ and different values$\sigma_1 = 0.3,0.7,1.0$.

Further considering the influence of noise amplitude on the transition path when the noise amplitude can be optimized, the results are shown in Fig.7. Fig.7(a) show the change of$\sigma_1$values saved per iteration 100 times when$\sigma_1$can be optimized, respectively. Fixed$\sigma_2 = 0.3$, the initial value of$\sigma_1$optimized by stochastic gradient descent method is taken as 0.1, and the stable value after 5000 iterations is about 0.2932. Fig.7(b) show the change of$\sigma_2$values saved per iteration 100 times whenσ_2 can be optimized, respectively. Fixed$\sigma_1 = 0.3$, the initial value of$\sigma_2$optimized by stochastic gradient descent method is taken as 1.0, and the stable value after 5000

iterations is about 0.3489.

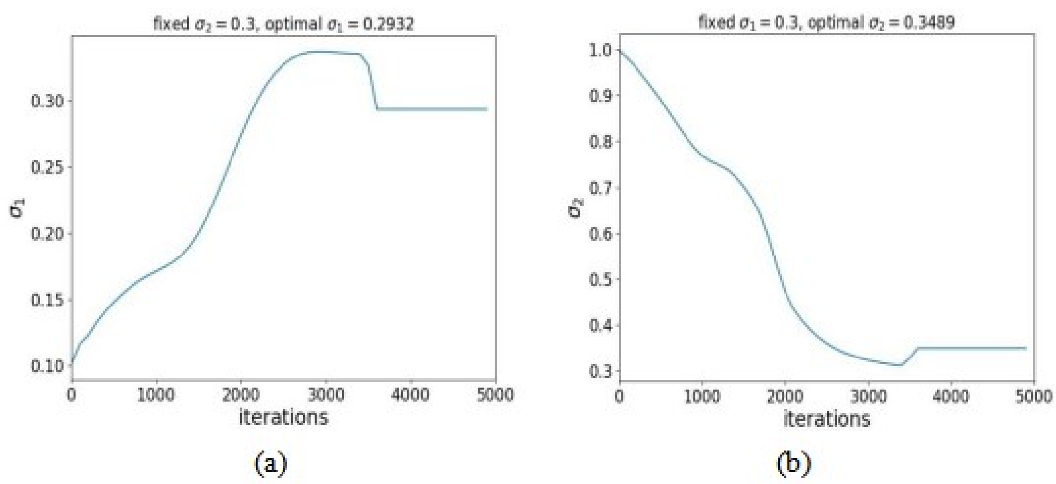

Figure 7 The convergence of noise amplitude with (a) trainable $\sigma_1$and (b) trainableσ_2.

3.2 The effect of transition time

This subsection is mainly divided into two parts. The first part discusses the minimum transition time corresponding to the target transition time$T \in [0,10]$, the results are shown in Fig.8. Fixing $\sigma_1 = 0.5, \sigma_2 = 0.3$, Fig.8 shows the corresponding most probable transition path at different time. In Fig. 8(a), the light red area represents the variance region. When different times$T$are fixed, we take 5 samples to draw the average trajectory. The threshold is taken as 10^{-4}, the minimum transition time corresponding to the first arrival at $10^{-4}$is$T^* \approx 0.18$. In Fig. 8(b), for the case$T = 0.15 < T^*$, because the transition time is not enough to jump from (-1,0) to (1,0), the corresponding loss in Fig.8(c) is also large. In Fig.8(d), for the case$T = 1 > T^*$, it can transition from (-1, 0) to (1, 0), and the corresponding loss in Fig. 8(e) is small, the most probable transition path corresponds to a double potential well situation.

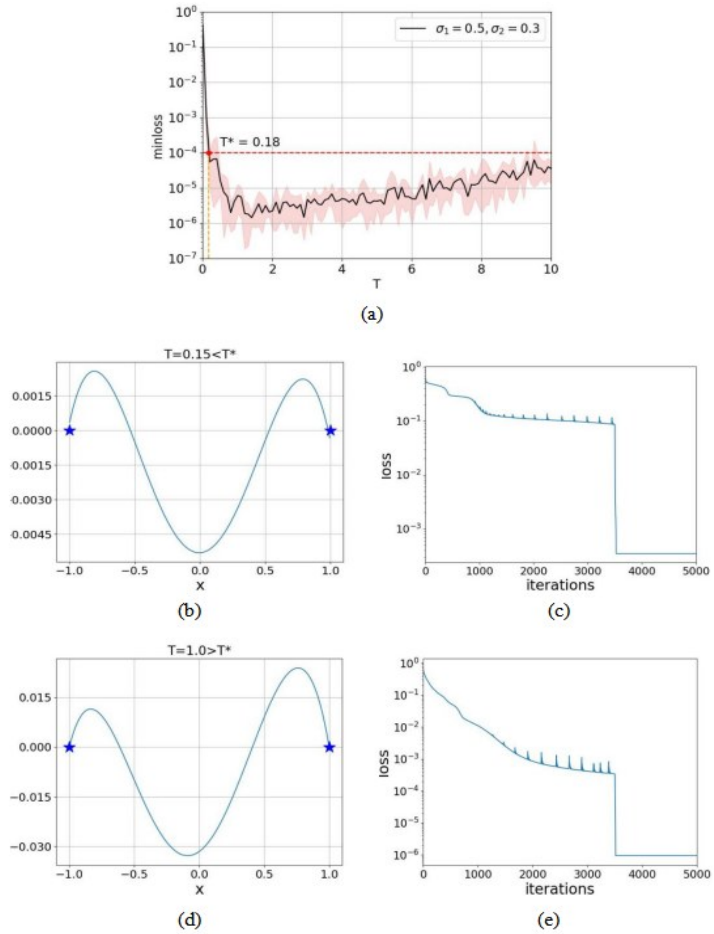

Figure 8(a) The minimum transition time corresponding to the target transition time $T \in [0,10], T^* = 0.18$.
(b) (c) Most probable transition path and loss for $T = 0.15 < T^*$. (d) (e) Most probable transition path and loss for $T = 1 > T^*$.

The second part discusses the transition path and loss at varying times and the same noise amplitude, as illustrated in Fig.9. The transition paths and loss are presented for $T = 2,3,10, \sigma_1 = 0.3, \sigma_2 = 0.5$. The results show that with the increase of time T, the transition path from $(-1,0)$ to $(1,0)$ gradually changes from arch to shape with two potential wells and one potential barrier.

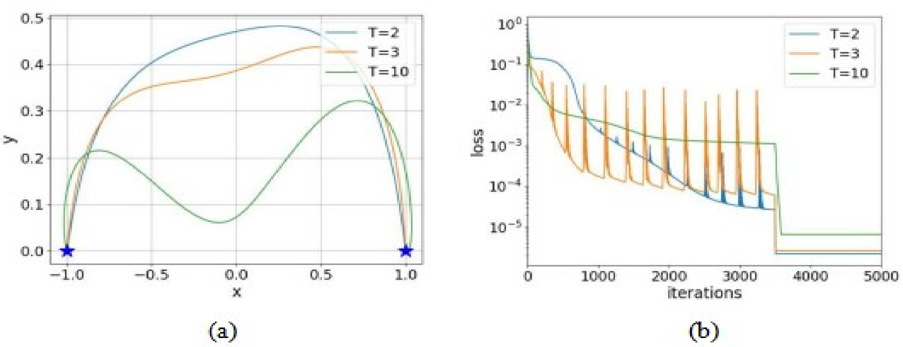

Figure 9 Transition path and loss with $T = 2,3,10$ and $\sigma_1 = 0.3, \sigma_2 = 0.5$.

4 Conclusion

In this paper, we propose a method to capture transition phenomena in nonlinear acoustic metamaterial models. By introducing the Onsager-Machlup functional theory, we quantify the transition dynamics and employ the PINNs method within the PyTorch framework, enhanced with a combined optimizer, to solve the Euler-Lagrange equation and identify the most probable transition path. Our evaluation of the convergence performance of various optimizers demonstrates that the combined optimization approach, AdamW + LBFGS, achieves significantly lower loss compared to using AdamW or SGD alone. Furthermore, we analyze transition phenomena under minimum transition time conditions and investigate the effects of noise fluctuations and transition time on transition dynamics. The findings reveal that noise can influence the direction of the most probable transition path, facilitating transitions between distinct manifold orientations. Additionally, we derive a critical threshold for the minimum transition time under fixed noise conditions. The results show that transitions cannot occur when the transition time is below this threshold.

About the Author

*Corresponding Author: Jinqian Feng.

References

[1] T. Chatterjee, K. K. Bera, A. Banerjee. Machine learning enabled quantification of stochastic active metadamping in acoustic metamaterials, J. Sound Vib. 567 (2023) 117938.

[2] Z. Yang, J. Mei, M. Yang. Membrane-types acoustics metamaterials with negative dynamic mass, Phys. Rev. Lett. 101 (2008) 204301.

[3] C. Liu, D. Yu, T. Li. Effects of neuronal morphology and time delay on inverse stochasic resonance in two-compartment neuron model, Phys. Lett. 493 (2024) 129268.

[4] öT. Lindstrm. On the stochastic engine of contagious diseases in exponentially growing populations, Nonlinear Anal Real World Appl. 77 (2024) 104045.

[5] E. Weinan, W. Ren, E. Vanden-Eijnden. Finite temperature string method for the study of rare events, Phys. Rev. B. 109 (2005) 6688–6693.

[6] Ingalls, P. Brian. Mathematical Systems Theory in Biology, Communications, Computation, and Finance, Springer. (2003).

[7] X. Li, T. Xing, J. Zhao. Broadband low frequency sound absorption using a monostable acoustic metamaterial, J. Acoust. Soc. Am.147 (2020) EL113–EL118.

[8] J. Hu, X. Chen, J. Duan. An Onsager-Machlup approach to the most probable transition pathway for a genetic regulatory network, Chaos. 32 (2022) 041103.

[9] W. Wei, J. Hu, J. Chen. Most Probable Transitions from Metastable to Oscillatory Regimes in a Carbon Cycle System, Chaos. 31 (2021) 121102.

[10] J. Liu, J. W. Crawford. Stability of an autocatalytic biochemical system in the presence of noise perturbations, Math Med Biol. 15 (1998) 339 –350.

[11] B. J. Zhang, T. Sahai, Y. M. Marzouk. A Koopman framework for rare event simulation in stochastic differential equations, J. Comput. Phys. 456 (2022) 111025.

[12] X. Wan, B. Zheng, G. Lin. An hp-adaptive minimum action method based on a posteriori error estimate, Commun Comput Phys. 23 (2018) 408 –439.

[13] M. I. Freidlin, A. D. Wentzell. Random Perturbations of Dynamical Systems, Springer. (2012).

[14] A. Dembo, O. Zeitouni. Large deviations techniques and their applications, Springer. (1993).

[15] M. Capitaine. Onsager-Machlup functional for some smooth norms on Wiener space, Probab Theory Relat Fields. 102 (1995) 189–201.

[16] W. Wei, X. Chen, J. Duan. An Optimal Control Method to Compute the Most Likely Transition Path for Stochastic Dynamical Systems with Jumps, Chaos. 32 (2022) 051102.

[17] L. Onsager, S. Machlup. Fluctuations and Irreversible Processes, Phys Rev. 91 (1953) 1505–1512.

[18] üD. Drr, A. Bach. The Onsager-Machlup function as Lagrangian for the most probable path of a diffusion process, Commun. Math. Phys. 60 (1978) 153–170.

[19] J. Hu, J. Chen. Transition pathways for a class of high dimensional stochastic dynamical systems with Levy noise, Chaos. 31 (2021) 063138.

[20] A. Ezoe, S. Morimoto, Y. Tanaka. Switching particle systems for foraging ants showing phase transitions in path selections, Physica A. 643 (2024) 129798.

[21] Y. Chao, J. Duan. The Onsager-Machlup function as Lagrangian for the most probable path of a jump-diffusion process, Nonlinearity. 32 (2019) 3715–3741.

[22] M. Raissi, P. Perdikaris and G.E. Karniadakis. Physics-informed neural networks: A deep learning framework for solving forward and inverse problems involving nonlinear partial differential equations, J. Comput. Phys. 378 (2019) 686–707.

[23] E. Weinan, W. Ren, E. Vanden-Eijnden. String method for the study of rare events, Phys. Rev. B. 66 (2002) 052301.

[24] M. Heymann, E.Vanden-Eijnden. The geometric minimum action method: A least action principle on the space of curves, Commun Pure Appl Math. 61 (2008) 1052– 1117.

[25] C. Emilio. First integral of the Euler-Lagrange equation and boundary conditions for stochastic processes: Bistable potential driven by colored noise, Phys. Lett. 223 (1996) 251–254.

[26] J. Feng, W. Xu, H. Rong. Stochastic responses of Duffing-Van der Pol vibro-impact system under additive and multiplicative random excitations, Int. J. Non Linear Mech. 41 (2009) 51–57.

[27] C. B. Kaio, Benedetti, B. Paulo, Goncalves, S. Lenci. Influence of uncertainties and noise on basins/attractors topology and integrity of Duffing oscillator, Int. J. Non Linear Mech. 159 (2024) 104594.

[28] X. Chen, J. Duan, J. Hu. Data-driven method to learn the most probable transition pathway and stochastic differential equations, Physica D. 443 (2023) 133559.